Human Molecular Genetics, 2013, Vol. 22, No. 15 **3112–3122**
doi:10.1093/hmg/ddt166
Advance Access published on April 10, 2013

The dual functions of the extreme N-terminus of TDP-43 in regulating its biological activity and inclusion formation

Yong-Jie Zhang, Thomas Caulfield, Ya-Fei Xu, Tania F. Gendron, Jaime Hubbard, Caroline Stetler, Hiroki Sasaguri, Ena C. Whitelaw, Shuyi Cai, Wing Cheung Lee and Leonard Petrucelli*

Department of Neuroscience, Mayo Clinic, 4500 San Pablo Road, Jacksonville, FL 32224, USA

Received January 15, 2013; Revised March 15, 2013; Accepted April 5, 2013

TAR DNA-binding protein-43 (TDP-43) is the principal component of ubiquitinated inclusions in amyotrophic lateral sclerosis (ALS) and the most common pathological subtype of frontotemporal dementia—frontotemporal lobar degeneration with TDP-43-positive inclusions (FTLD-TDP). To date, the C-terminus of TDP-43, which is aggregation-prone and contains almost all ALS-associated mutations, has garnered much attention while the functions of the N-terminus of TDP-43 remain largely unknown. To bridge this gap in our knowledge, we utilized novel cell culture and computer-assisted models to evaluate which region(s) of TDP-43 regulate its folding, self-interaction, biological activity and aggregation. We determined that the extreme N-terminus of TDP-43, specifically the first 10 residues, regulates folding of TDP-43 monomers necessary for proper homodimerization and TDP-43-regulated splicing. Despite such beneficial functions, we discovered an interesting dichotomy: full-length TDP-43 aggregation, which is believed to be a pathogenic process, also requires the extreme N-terminus of TDP-43. As such, we provide new insight into the structural basis for TDP-43 function and aggregation, and we suggest that stabilization of TDP-43 homodimers, the physiologically active form of TDP-43, may be a promising therapeutic strategy for ALS and FTLD-TDP.

INTRODUCTION

Inclusions of TAR DNA-binding protein of 43 kDa (TDP-43) are a histological hallmark of frontotemporal lobar degeneration with TDP-43-positive inclusions (FTLD-TDP) and amyotrophic lateral sclerosis (ALS) (1,2). While TDP-43 predominantly localizes to the nucleus under normal conditions, a substantial loss of nuclear TDP-43 and aberrant cytoplasmic TDP-43 inclusions marks neurons affected by disease. In such cases, TDP-43 exhibits a disease-specific biochemical signature, which includes its ubiquitination, phosphorylation and truncation (1,2). As a highly conserved heterogeneous nuclear ribonucleoprotein (hnRNP), TDP-43 plays roles in the regulation of DNA transcription, RNA splicing and degradation, as well as microRNA biogenesis and processing (3). TDP-43 contains four functional domains, which include a nuclear localization signal (NLS) and two RNA recognition motifs (RRMs) within the N-terminal half of the protein, as well as a nuclear export signal (NES) and a glycine-rich region in the C-terminal half. The NLS and NES regulate the shuttling of TDP-43 between the nucleus and the cytoplasm (4), while the RRM1 and RRM2 are responsible for binding to nucleic acids, such as UG repeats (5,6). The glycine-rich region mediates protein–protein interactions between TDP-43 and other hnRNP members (7). Since the C-terminal region of TDP-43 harbors almost all known ALS-associated TDP-43 mutations (8–15), and contains Q/N-rich domains that promote TDP-43 aggregation (16,17), research has mostly focused on the C-terminal region of TDP-43. As a result, the functions of TDP-43's N-terminal region remain largely unknown.

We previously shed light on the importance of the N-terminus of TDP-43: we have shown that deletion of the

*To whom correspondence should be addressed at: Department of Neuroscience, Mayo Clinic, 4500 San Pablo Road, Jacksonville, FL 32224, USA. Tel: +1 904 953 2855; Fax: +1 904 953 7370; Email: petrucelli.leonard@mayo.edu

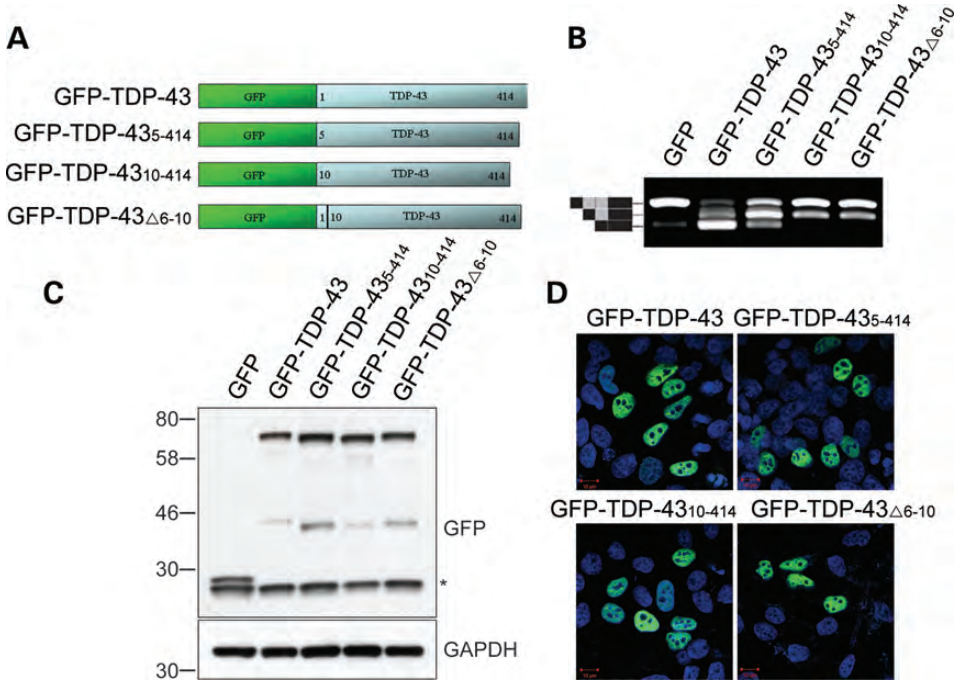

Figure 1. The first 10 N-terminal residues of TDP-43 are required for its biological activity. (**A**) Schematic representation of N-terminal GFP-tagged TDP-43 fragments co-transfected into HeLa cells with the *CFTR* mini-gene reporter construct. (**B**) Examination of *CFTR* exon 9 skipping by RT–PCR shows that, compared with exon 9-containing products in cells expressing GFP (top band), expression of GFP-TDP-43 significantly promotes exon 9 skipping (bottom band). In contrast, the N-terminal deleted TDP-43 fragments show a decreased ability to promote exon 9 exclusion. (**C**) Western blot analysis using an anti-GFP antibody confirmed that the examined GFP-tagged TDP-43 products were expressed at similar levels (* represents a nonspecific band). (**D**) Similar to full-length TDP-43, the examined TDP-43 fragments localized to the nucleus (Scale bar 10 μm).

first 75 amino acid residues of TDP-43 significantly reduces its biological activity, as measured using a cellular cystic fibrosis transmembrane conductance regulator (*CFTR*) exon 9 splicing assay (14). Moreover, we and others have demonstrated that TDP-43 molecules interact and their binding to one another leads to homodimer formation *in vitro* and within cells (14,15,18–20). Our data further indicated that deletion of the first 75 residues of TDP-43 dramatically reduces this self-interaction (14). Based on these findings, we sought to further define the region(s) of TDP-43 critical for its biological activity and self-interaction. The findings of the present study, emerging from both cellular models and computer-assisted modeling of TDP-43, suggest that the first 10 amino acid residues of TDP-43 are essential for proper monomer folding, homodimer formation and splicing activity. Indeed, deletion of these 10 residues, and even mutations of key residues within this sequence, impairs TDP-43 homodimer formation and result in the loss of TDP-43-regulated splicing. In contrast to the beneficial role of these 10 N-terminal residues in regulating TDP-43 function, our results also indicate that the extreme N-terminus of TDP-43 regulates full-length TDP-43 inclusion formation. Our findings provide greater insight into the dual functions of the extreme N-terminal region of TDP-43 in regulating TDP-43 conformation which influences its biological activity and inclusion formation. The stabilization of physiologically active TDP-43 homodimers to prevent their oligomerization may thus be a therapeutic strategy meriting consideration for the treatment of ALS and FTLD-TDP.

RESULTS

The first 10 N-terminal residues of TDP-43 are required for its splicing activity

One of the first recognized biological activities of TDP-43 was its ability to promote skipping of *CFTR* exon 9 (21), and it is now recognized that TDP-43 influences the splicing pattern of many mRNAs (22,23). As mentioned, we have demonstrated that deletion of the first 75 residues of TDP-43 (TDP-43$_{76-414}$) significantly reduces its splicing activity (14). To further define the region(s) required for TDP-43 function, we generated various expression vectors encoding N-terminal deleted fragments of TDP-43 tagged with enhanced green fluorescence protein (GFP-TDP-43$_{5-414}$, GFP-TDP-43$_{10-414}$, GFP-TDP-43$_{\Delta 6-10}$, GFP-TDP-43$_{15-414}$, GFP-TDP-43$_{31-414}$, GFP-TDP-43$_{46-414}$ and GFP-TDP-43$_{61-414}$; Fig. 1A and Supplementary Material, Fig. S1A). HeLa cells were co-transfected to overexpress individual TDP-43 fragments and a *CFTR* mini-gene reporter construct. Two days after transfection, *CFTR* exon 9 skipping was examined by reverse-transcription PCR (RT–PCR) followed by visualization of transcripts that include (top band) or exclude (bottom band) exon 9 on an agarose gel (Fig. 1B and Supplementary Material, Fig. S1B). Expression of GFP-TDP-43 markedly increased exon 9 exclusion compared with the minor expression of *CFTR* exon 9 exclusion products present in cells expressing only GFP. Expression of all N-terminally truncated TDP-43 fragments led to a substantial decrease in exon 9 exclusion compared with full-length TDP-43 (Fig. 1B and Supplementary Material, Fig. S1B), despite comparable levels of expression (Fig. 1C and

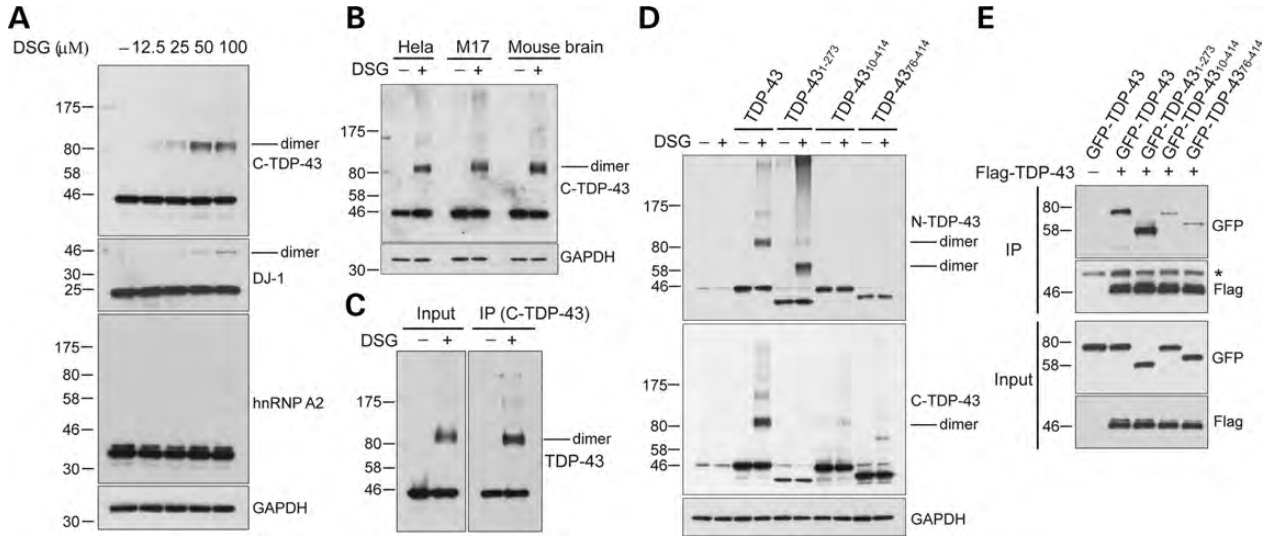

Figure 2. The first 10 N-terminal residues of TDP-43 are required for the formation of a functional TDP-43 homodimer. (**A**) Live HEK293T cells were treated with DSG, a homobifunctional NHS-ester cross-linking reagent used to study native protein structures. Western blot analysis of endogenous TDP-43 using an antibody toward the C-terminus of TDP-43 (C-TDP-43) revealed that TDP-43 in non-cross-linked cells migrates at the expected molecular weight of a monomer (~45 kDa), whereas TDP-43 in DSG-treated cells migrates at the expected molecular weight of a homodimer (~90 kDa). Blots were also probed for: DJ-1, which is known to form homodimers; hnRNP A2, a protein that can interact with TDP-43; and GAPDH, to confirm equal loading among wells. (**B**) TDP-43 homodimers are also present in DSG-treated HeLa cells, M17 neuroblastoma cells and mouse brain lysate. (**C**) Immunoprecipitation of TDP-43 from DSG-treated cell lysates pulls down TDP-43 homodimers. (**D**) Similar to endogenous TDP-43, ectopic TDP-43$_{WT}$ or a TDP-43 C-terminal deletion fragment (TDP-43$_{1-273}$) form homodimers. In contrast, N-terminal deleted TDP-43 fragments (TDP-43$_{10-414}$ or TDP-43$_{76-414}$) do not form homodimers in DSG-treated cells. Note that the high-molecular weight material in DSG-treated cells likely consists of complexes formed of TDP-43 homodimers and bound DNA substrates. (**E**) Co-immunoprecipitation experiments revealed that GFP-TDP-43 and GFP-TDP-43$_{1-273}$ bind strongly to Flag-TDP-43. In contrast, GFP-TDP-43$_{10-414}$ and GFP-TDP-43$_{76-414}$ only weakly interact with Flag-TDP-43 (* represents a nonspecific IgG band).

Supplementary Material, Fig. S1C) and nuclear localization (Fig. 1D and Supplementary Material, Fig. S1D). Similar results were observed when comparing splicing activity between non-tagged full-length TDP-43 and N-terminally deleted fragments (TDP-43$_{5-414}$ and TDP-43$_{10-414}$; Supplementary Material, Fig. S1E). Note that, in contrast to the partial reduction in exon 9 skipping caused by TDP-43$_{5-414}$, exon 9 skipping was completely abolished upon expression of TDP-43$_{10-414}$ and of other tested fragments (Fig. 1B, Supplementary Material, Fig. S1B and E), suggesting that the first 10 amino acid residues of TDP-43 are critical for its splicing activity.

The first 10 N-terminal residues of TDP-43 are required for the formation of a functional TDP-43 homodimer

Several groups, including our own, have reported that TDP-43 molecules interact and their binding to one another results in the formation of homodimers (14,15,18–20). We thus investigated whether the first 10 N-terminal residues of TDP-43 mediate this self-interaction and whether formation of TDP-43 homodimers is critical for TDP-43 splicing activity. Intact, live HEK293T cells were treated with membrane-permeable disuccinimidyl glutarate (DSG), a homobifunctional NHS-ester cross-linking reagent widely used to study native protein structures (24–28). Treating cells with DSG prior to lysis allowed the preservation of TDP-43 structure and protein interactions found under physiological conditions. Upon analysis of TDP-43 by denaturing SDS–PAGE, it was observed that TDP-43 in non-cross-linked cells migrated at the expected molecular weight of a monomer (~45 kDa), whereas the SDS-stable TDP-43 in DSG-treated cells migrated at the expected molecular weight of a homodimer (~90 kDa) (Fig. 2A and Supplementary Material, Fig. S2A). The ~90 kDa band immunoreactive for TDP-43 was not immunoreactive for hnRNP A2, a protein known to interact with TDP-43 (7,14) (Fig. 2A), suggesting that there is no significant cross-linking between TDP-43 and other proteins under these conditions. We found that treating purified recombinant TDP-43 protein with DSG also results in TDP-43 homodimerization and the generation of a 90 kDa band, further supporting the notion that the 90 kDa band consists of TDP-43 homodimers (Supplementary Material, Fig. S2A). In addition, TDP-43 immunoprecipitation studies using lysates from DSG-treated and non-treated HEK293T cells confirmed the existence of TDP-43 homodimers in live cells (Fig. 2C). Such TDP-43 homodimers were similarly observed in DSG-treated Hela cells, neuroblastoma M17 cells and mouse brain (Fig. 2B).

Note that levels of the TDP-43 homodimers in cells increased dose-dependently upon DSG treatment (Fig. 2A and Supplementary Material, Fig. S2A), and TDP-43 retained its normal nuclear localization (Supplementary Material, Fig. S2B). Consistent with previous findings (24,29), DSG treatment also stabilized DJ-1 homodimers, the native form of DJ-1 in cells (26,30,31), validating our experimental conditions were sufficient to stabilize native protein structures. Indeed, high-dose DSG treatment (1000 μM) was found to significantly increase levels of TDP-43 and DJ-1 homodimers while simultaneously decreasing their monomeric forms (Supplementary Material, Fig. S2A). Since the low dose of DSG (100 μM) is expected to minimize nonspecific cross-linking

between TDP-43 and other proteins and its DNA substrates, this dose was used in subsequent studies. Taken together, our cross-linking data are consistent with previous studies (14,15,18–20) and support the notion that native TDP-43 homodimers exist in cells.

Next, to determine whether the extreme N-terminus of TDP-43 modulates homodimer formation, we generated expression vectors encoding untagged N-terminal deleted TDP-43 fragments (TDP-43_{10-414} and TDP-43_{76-414}) or a C-terminal deleted fragment (TDP-43_{1-273}). Cells were transfected with these constructs following knockdown of endogenous TDP-43 by RNA interference (siRNA). Following DSG treatment to cross-link TDP-43, cell homogenates were analyzed by western blot as above. Similar to endogenous TDP-43, ectopically expressed wild-type TDP-43 (TDP-43_{WT}) and TDP-43_{1-273} formed homodimers in cells (Fig. 2D); however, TDP-43 products lacking N-terminal residues (TDP-43_{10-414} or TDP-43_{76-414}) did not (Fig. 2D). To further confirm the extreme N-terminus of TDP-43 regulates its self-interaction, co-immunoprecipitation experiments were performed in which HEK293T cells were cotransfected with Flag-TDP-43 and either GFP-TDP-43, GFP-TDP-43_{1-273}, GFP-TDP-43_{10-414}, or GFP-TDP-43_{76-414}. Immunoprecipitation of Flag-TDP-43 followed by probing for GFP revealed that Flag-TDP-43 bound strongly to GFP-TDP-43 and to the C-terminal deletion product GFP-TDP-43_{1-273}. In contrast, GFP-TDP-43_{10-414} and GFP-TDP-43_{76-414} only weakly interacted with Flag-TDP-43, despite comparable expression levels in cell lysates, suggesting that the N-terminus of TDP-43 regulates homodimer formation (Fig. 2E). Of importance, TDP-43_{10-414} and TDP-43_{76-414} also lost their ability to regulate splicing of the *CFTR* mini-gene (Supplementary Material, Fig. S2C), as did the GFP-tagged N-terminal TDP-43 deletion products shown above (Fig. 1), despite their normal nuclear localization (Supplementary Material, Fig. S2D). These findings suggest that the extreme N-terminus of TDP-43 is required for both TDP-43 homodimer formation and TDP-43-regulated splicing in cells.

Finally, since it has been reported that RNA is required for the interaction of TDP-43 and ATXN2 (32), we examined whether formation of TDP-43 homodimers is similarly dependent on its DNA/RNA binding activity. To this end, five conserved Phe residues (147, 149, 194, 229 and 231) in the RRM domains of TDP-43 were mutated to Leu (TDP-43_{5F-L}), which has previously been shown to abolish the ability of TDP-43 to bind DNA/RNA *in vitro* and within cells (6,32,33). We observed that TDP-43_{5F-L} formed homodimers to the same extent as TDP-43_{WT} in DSG-treated cells (Supplementary Material, Fig. S2E), suggesting that the formation of TDP-43 homodimers is independent of DNA/RNA binding.

Arg6, Val7, Thr8 and Glu9 are required for proper folding and homodimerization of TDP-43

To understand how the structure of the extreme N-terminus of TDP-43 affects homodimer formation, computer-assisted modeling was utilized. The human TDP-43 protein contains four distinct regions: N-terminal region, RRM1, RRM2 domain, and C-terminal region (Fig. 3A). Our modeling of a full-length TDP-43 monomer, bound or not to DNA/RNA, provided structures in closed and open conformations (Fig. 3A and Supplementary Material, Fig. S3). While the structures of the extreme N-terminal region of TDP-43 are identical in both conformations, the closed conformation was used for the present study given its greater stability (Fig. 3A and Supplementary Material, Movie S1). Overall, our model showed that the structural arrangement of the TDP-43 protein is quite distinct and flexible in certain regions. The structure of the N-terminus has a minor loop/flexible region between the N-terminus and RRM1 around residues 101–106. The RRM1 and RRM2 domains are relatively fixed in arrangement to each other, while a larger loop/flexible region exists between RRM2 and the C-terminus domain at residues 273–280.

Since our data indicated that the N-terminus of TDP-43 are required for its self-interaction and splicing activity, we focused our attention on the structure of this region. As shown in Figure 3A, the N-terminal region has several β-sheet-like motifs within the first 60 amino acid residues, punctuated by key Pro residues at positions 15 and 19. Forming portions of the inter-strand β-sheet-like structure are residues 6–13 that interact with residues 35–39, as well as residues 39–45 that interact with residues 52–57. Between residues 25 and 32 is a short helical segment that connects across the β-sheet-like structure. Likewise, between residues 57 and 62 is a brief helical segment adjoining the β-sheet minor domain with the final helical element (Asp89-Val100) before the RRM1 domain begins around residue 101. Of particular relevance to the current study, there are strong intra-strand interactions that form in the initial 11 amino acid residues of TDP-43. Specifically, residues Arg6, Val7, Thr8 and Glu9 form strong intra-strand interactions with Phe35 (Fig. 3B and Supplementary Material, Movie S1). Therefore, we additionally characterized the structure of TDP-43_{10-414} (deletion of residues 2–9), and observed that, compared with full-length TDP-43 (Supplementary Material, Movie S2), the absence of residues 2–9 in TDP-43_{10-414} resulted in a loss of domain structure integrity and subsequent uncoiling of that region of the protein (Supplementary Material, Movie S3).

In addition to evaluating the role of the N-terminus in maintaining proper folding of the TDP-43 monomer, we investigated whether the extreme N-terminus of TDP-43 is crucial for homodimer formation. Based on the predictions from YASARA and PRIME on likely regions of dimerization, we derived three optimal models (Supplementary Material, Fig. S4 and Supplementary Material, Table S1). Examination of key residues interacting between the monomers in all three models clearly showed that the amino acid residues in the N-terminus of TDP-43 are critical for interactions necessary to maintain the structure of the homodimer interface. Thus, computer modeling of TDP-43 monomers and homodimers highlights that residues in the N-terminus of TDP-43 are critical for both proper monomer folding and homodimerization.

In light of the putative role of residues Arg6, Val7, Thr8 and Glu9 in monomeric TDP-43 folding, we tested whether mutating these residues to Gly would consequently affect TDP-43 homodimer formation and function. Based on computer-modeling, we found that, compared with TDP-43_{WT} (Supplementary Material, Movie S4), TDP-43_{R6GV7G} and TDP-$43_{R6GV7GT8GE9G}$ mutants are less stable in the first 40 amino acids (Supplementary Material, Movies S5 and S6). As a result, our data suggest proper monomer folding, and thereby homodimer formation of these TDP-43 species may be impaired.

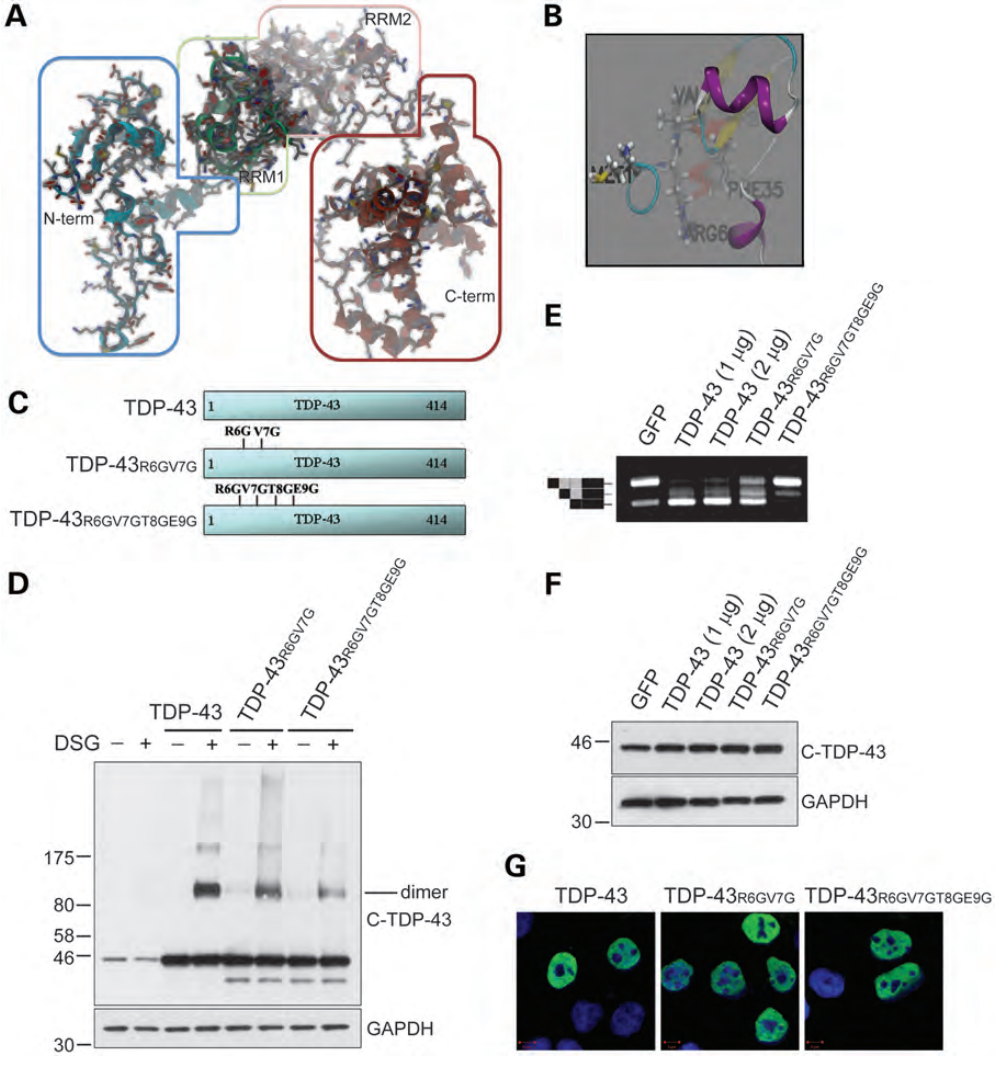

Figure 3. Arg6, Val7, Thr8 and Glu9 are required for TDP-43 homodimerization and splicing regulation. (**A**) Computer-assisted modeling of full-length monomeric TDP-43 in the closed conformation showing TDP-43's four distinct regions: N-terminal domain, RRM1 domain, RRM2 domain and C-terminal domain. (**B**) The interactions of Arg6, Val7, Thr8 and Glu9 with Phe35 stabilize the N-terminal β-sheet-like structures within the N-terminal region. (**C**) Schematic representation of untagged TDP-43 mutants used for transfection into HEK293T cells. (**D**) Compared with TDP-43_{WT}, homodimer formation in DSG-treated cells is impaired upon expression of TDP-43_{R6GV7G} and TDP-$43_{R6GV7GT8GE9G}$, as assessed by western blot using an antibody toward the C-terminus of TDP-43 (C-TDP-43). (**E**) Similarly, TDP-43_{R6GV7G} and TDP-$43_{R6GV7GT8GE9G}$ do not effectively promote exon 9 exclusion of the *CFTR* mini-gene reporter, as does TDP-43_{WT}. (**F**) Western blot analysis confirmed that the examined TDP-43 products were expressed at similar levels. (**G**) The TDP-43 mutants exhibit normal nuclear distribution similar to TDP-43_{WT} (Scale bar 10 μm).

To examine this in cells, HEK293T cells were transfected to overexpress TDP-43_{R6GV7G} or TDP-$43_{R6GV7GT8GE9G}$ under the conditions of endogenous TDP-43 knockdown (schematic of expression constructs shown in Fig. 3C). As above, DSG treatment to cross-link TDP-43 led to the formation of TDP-43 homodimers in cells expressing TDP-43_{WT} (Fig. 3D). However, the levels of cross-linked homodimers were significantly decreased in cells overexpressing TDP-43_{R6GV7G} or TDP-$43_{R6GV7GT8GE9G}$ (Fig. 3D), indicating that disruption of the N-terminal β-strand structure of TDP-43 inhibits homodimer formation. In addition, compared with the levels of *CFTR* exon 9 exclusion in cells transfected with TDP-43_{WT}, TDP-43 mutants partially (TDP-43_{R6GV7G}) or completely (TDP-$43_{R6GV7GT8GE9G}$) lost their ability to regulate splicing (Fig. 3E), despite comparable levels of expression (Fig. 3F) and normal nuclear localization (Fig. 3G). Of note, the splicing activity of TDP-43 correlated with levels of TDP-43 homodimers, thus supporting the notion that dimerization is integral to the biological function of TDP-43, at least with respect to its role in regulating certain splicing events. Taken together, these findings provide additional evidence that the extreme N-terminal region of TDP-43 is required to maintain its structure and splicing activity.

The extreme N-terminus of TDP-43 regulates the aggregation of full-length TDP-43

To investigate the potential role of TDP-43's extreme N-terminus in disease pathogenesis, we examined whether the first 10 amino acid residues of TDP-43 are necessary for the aggregation of

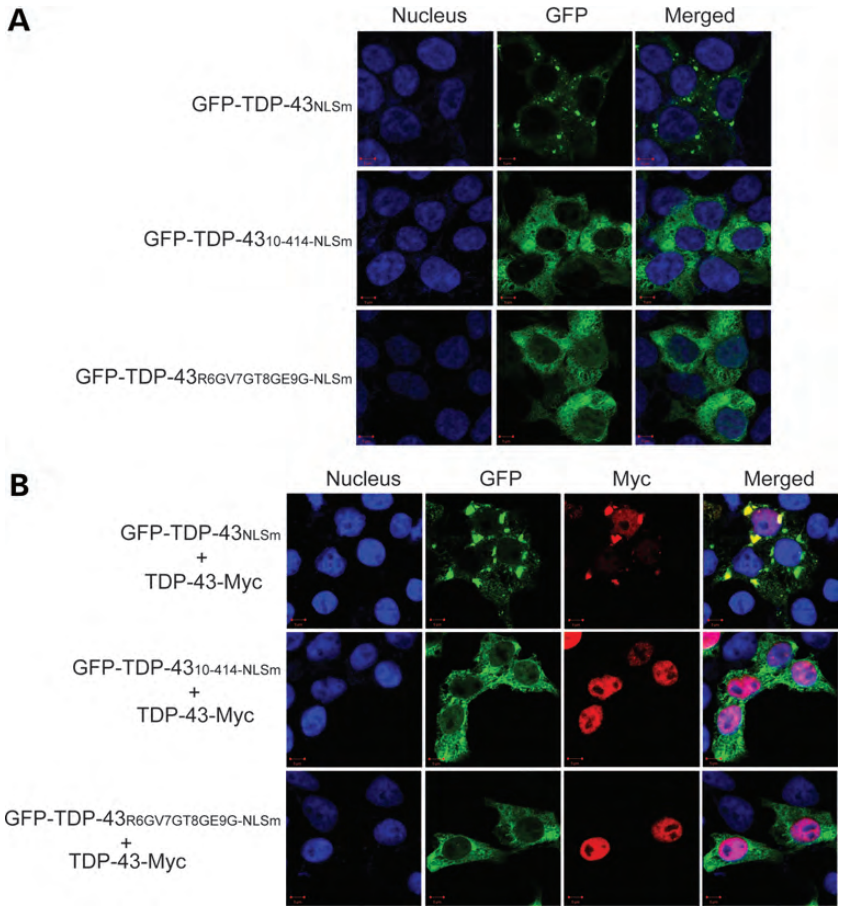

Figure 4. The extreme N-terminus of TDP-43 is required for aggregation of full-length TDP-43. (**A**) The ectopic expression of GFP-TDP-43_{NLSm} leads to the formation of cytoplasmic TDP-43 inclusions in cells, as examined by confocal fluorescence microscopy. In contrast, deletion of the extreme N-terminus of TDP-43, or mutations in key N-terminal residues, impairs inclusion formation such that GFP-TDP-$43_{10-414\text{-}NLSm}$ and GFP-TDP-$43_{R6GV7GT8GE9G\text{-}NLSm}$ remain diffusely localized to the cytoplasm (Scale bar 5 μm). (**B**) The cytoplasmic TDP-43 inclusions composed of GFP-TDP-43_{NLSm} (green) sequester Myc-tagged TDP-43_{WT} in cytoplasmic inclusions (red). In contrast, TDP-43_{WT}-Myc remains in the nucleus of cells expressing GFP-TDP-$43_{10-414\text{-}NLSm}$ or GFP-TDP-$43_{R6GV7GT8GE9G\text{-}NLSm}$ (Scale bar 5 μm).

full-length TDP-43. To this end, we utilized expression vectors encoding full-length TDP-43, TDP-43_{10-414} or TDP-$43_{R6GV7GT8GE9G}$ containing mutations (K82A, R83A, K84A) in the NLS (GFP-TDP-43_{NLSm}, GFP-TDP-$43_{10-414\text{-}NLSm}$ and GFP-TDP-$43_{R6GV7GT8GE9G\text{-}NLSm}$). Consistent with previous reports (4,32,34), ectopic expression of GFP-TDP-43_{NLSm} led to the formation of cytoplasmic TDP-43 inclusions in cells, as examined by confocal fluorescence microscopy (Fig. 4A). In contrast, the majority of GFP-TDP-$43_{10-414\text{-}NLSm}$ and GFP-TDP-$43_{R6GV7GT8GE9G\text{-}NLSm}$ was diffusely distributed in the cytoplasm (Fig. 4A).

Given that cytoplasmic TDP-43 inclusions sequester full-length, normally nuclear, TDP-43 (4), we next co-transfected cells to overexpress Myc-tagged TDP-43_{WT} and either GFP-TDP-43_{NLSm}, GFP-TDP-$43_{10-414\text{-}NLSm}$ or GFP-TDP-$43_{R6GV7GT8GE9G\text{-}NLSm}$ (Fig. 4B). TDP-43_{WT}-Myc localized primarily to the nucleus when overexpressed alone, but was sequestered into cytoplasmic inclusions when co-expressed with GFP-TDP-43_{NLSm} (Fig. 4B). Conversely, TDP-43_{WT}-Myc maintained its nuclear distribution in cells overexpressing diffuse, cytosolic GFP-TDP-$43_{10-414\text{-}NLSm}$ or GFP-TDP-$43_{R6GV7GT8GE9G\text{-}NLSm}$ (Fig. 4B), again displaying that, under conditions that mimic disease, the first 10 residues of TDP-43 are necessary for the sequestration and aggregation of full-length TDP-43.

Finally, we sought to determine whether GFP-TDP-43_{NLSm}, GFP-TDP-$43_{10-414\text{-}NLSm}$ and GFP-TDP-$43_{R6GV7GT8GE9G\text{-}NLSm}$ form aggregates and impair neuronal outgrowth in primary cultured neurons. We observed that transducing primary cortical neurons with rAAV1-GFP-TDP-43_{NLSm} for 5 days resulted in the formation of cytoplasmic inclusions within the soma and neurites (Fig. 5A). In contrast, the expression of GFP-TDP-$43_{10-414\text{-}NLSm}$ or GFP-TDP-$43_{R6GV7GT8GE9G\text{-}NLSm}$ resulted in the diffuse distribution of TDP-43 in neurons (Fig. 5A). Notably, compared with GFP expression, expression of GFP-TDP-43_{NLSm} resulted in a reduction of neurite outgrowth (Fig. 5A and B). However, neurite outgrowth was not affected by GFP-TDP-$43_{10-414\text{-}NLSm}$ and GFP-TDP-$43_{R6GV7GT8GE9G\text{-}NLSm}$ expression (Fig. 5A and B), suggesting that impaired neurite outgrowth is caused by cytoplasmic TDP-43 inclusions but not diffusely expressed cytoplasmic TDP-43.

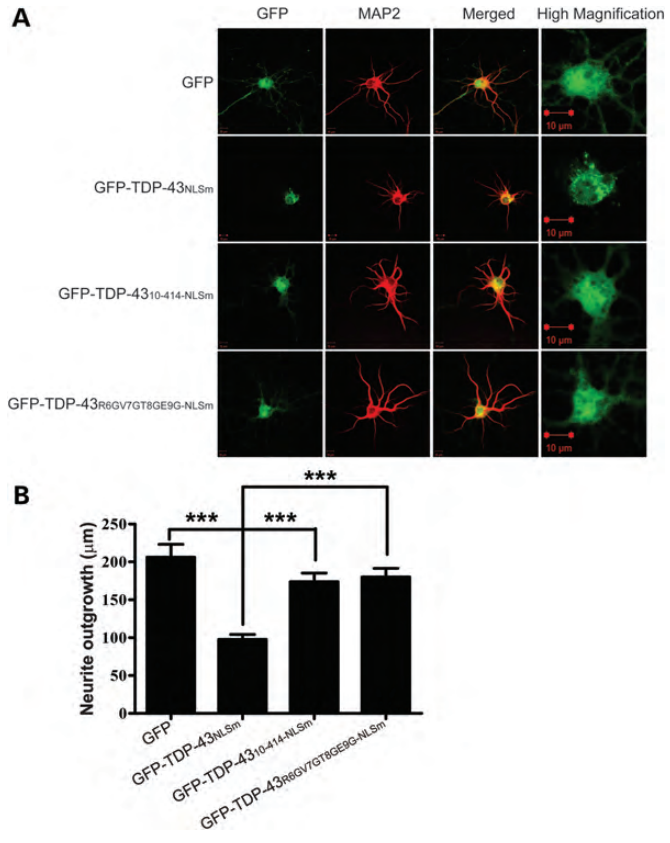

Figure 5. The extreme N-terminus of TDP-43 mediates full-length TDP-43 aggregation. (**A**) At day *in vitro* 4, primary cortical neurons plated on coverslips were transduced with rAAV1-GFP, rAAV1-GFP-TDP-43_{NLSm}, rAAV1-GFP-TDP-$43_{10-414\text{-}NLSm}$ or GFP-TDP-$43_{R6GV7GT8GE9G\text{-}NLSm}$. Five days post-infection, cells were immunostained for the neuronal marker, microtubule-associated protein 2 (MAP2), and coverslips were examined by fluorescence confocal microscopy. Green = GFP; red = MAP2; blue = Hoechst (nuclear stain). Exogenously expressed TDP-43_{NLSm} formed cytoplasmic TDP-43 inclusions in neurons. In contrast, TDP-$43_{10-414\text{-}NLSm}$ and TDP-$43_{R6GV7GT8GE9G\text{-}NLSm}$ showed diffuse distribution similar to GFP (Scale bar 10 μm). (**B**) The cytoplasmic TDP-43 inclusions composed of TDP-43_{NLSm} impaired neurite outgrowth. Data from three separate experiments were analyzed by one-way analysis of variance followed by Tukey's *post-hoc* analysis (***$P < 0.001$).

DISCUSSION

Since the discovery of TDP-43 as the major component of ubiquitinated inclusions in FTLD-TDP and ALS patients (1,2), much research has aimed to better understand the normal functions of TDP-43 and its role in disease pathogenesis. The accumulation of cytoplasmic TDP-43 inclusions may be toxic to neurons, while abnormal post-translational modifications of TDP-43 and its sequestration into inclusions are expected to result in a loss of TDP-43 function. Functions of TDP-43 include the regulation of DNA transcription, microRNA processing, as well as RNA splicing (3). With regards to the latter, we previously demonstrated that the first 75 residues of TDP-43 are required for the protein's normal biological activity (14). The purpose of the present study was to hone in on the specific N-terminal region(s) required for a proper TDP-43 structure, function and aggregation. Our findings suggest that the first 10 amino acid residues of TDP-43 are critical for TDP-43 monomer folding and thus homodimerization, which is necessary for TDP-43-regulated splicing. The extreme N-terminus of TDP-43, however, may function as a double-edged sword; in addition to its vital role in regulating TDP-43 function, the same region is necessary for full-length TDP-43 inclusion formation. A better understanding of what factors may tip the balance between normal TDP-43 homodimerization and TDP-43 oligomerization is an area meriting more attention.

The extreme N-terminus of TDP-43 stabilizes its monomeric structure and mediates TDP-43 homodimerization

Upon evaluating the biological activity of a series of N-terminally deleted TDP-43 products using a cellular *CFTR* slicing assay, we determined that the first 10 amino acid residues of this protein are critical for its role in regulating splicing. These same 10 residues are required for TDP-43 monomer folding, and homodimerization within cells, as assessed by DSG-induced cross-linking to preserve the integrity of TDP-43 physiological structures. SDS-stable TDP-43 homodimers were observed in various human cell lines and in mouse brain, as well as *in vitro* using recombinant TDP-43. These results are consistent with previous studies, demonstrating that TDP-43 interacts with itself to form a homodimer *in vitro* and in cells (14,15,18–20). While TDP-43_{WT} and a C-terminal deleted TDP-43 fragment (TDP-43_{1-273}) formed homodimers in cells, N-terminal deleted TDP-43 fragments (TDP-43_{10-414} or TDP-43_{76-414}) showed markedly impaired homodimer formation. In addition, co-immunoprecipitation studies further revealed that TDP-43 homodimerization is dependent on the N-terminal region of TDP-43. Of interest, compared with TDP-43_{WT}, both the C-terminal deleted fragment (TDP-43_{1-273}) and the N-terminal deleted fragments (TDP-43_{10-414} or TDP-43_{76-414}) lost their ability to promote *CFTR* exon 9 exclusion. This finding is in agreement with previous reports, showing that the glycine-rich C-terminal domain of TDP-43 mediates its binding to hnRNPA/B proteins and the formation of hnRNP-rich complexes necessary for TDP-43 activity (7). Of importance, our data strongly suggest that the active form of TDP-43, at least when regulating splicing, is a homodimer.

The novel use of computer-assisted modeling of TDP-43 allowed us to highlight the importance of the N-terminal region in maintaining monomeric and homodimeric TDP-43 structures. Indeed, these models revealed that the extreme N-terminus of TDP-43 is critical for proper monomeric TDP-43 folding. Deletion of residues 2–9 (TDP-43_{10-414}) results in a loss of domain structure integrity and subsequent uncoiling of that region of the protein, and therefore destabilizes the β-sheets characteristic of the first 60 amino acids. Since the extreme N-terminal region of TDP-43 is important for monomer folding, changing its structure would disrupt the proper folding, and subsequently alter homodimer formation. To evaluate the importance of the extreme N-terminus for the TDP-43 structure in a cellular model, cells were made to express TDP-43 mutated at residues 6–9, TDP-$43_{R6GV7GT8GE9G}$. As expected, these mutations abolished TDP-43 homodimer

formation, resulting in the loss of TDP-43-regulated *CFTR* exon 9 splicing, which further validated that the extreme N-terminus of TDP-43 is critical for stabilizing TDP-43 in its active, homodimeric conformation. TDP-43 homodimer models revealed that key N-terminal residues are also critical to stabilize the interactions between the two monomers forming the homodimer. Consistent with these findings, a recent study has shown that the N-terminus of TDP-43 is an ordered structure and acts as an oligomerization domain (35). Although our computer-based structural models need to be confirmed by TDP-43 crystal structures, our findings provide insight into understanding the relationship between physiological TDP-43 structures and biological activity.

The N-terminus of TDP-43 and disease pathogenesis

It is widely believed that the glycine-rich C-terminal domain of TDP-43, which also contains prion-related domains rich in Glu and Asp residues, is aggregation-prone and crucial for inclusion formation (16,17). We and others have shown that C-terminal fragments of TDP-43 (e.g. TDP-$43_{220-414}$) readily aggregate in various cell lines (13–15). In contrast, full-length, nuclear TDP-43 is much less prone to aggregate in cultured cells. Nonetheless, preventing the nuclear import of full-length TDP-43 by mutating the NLS causes it to aggregate into insoluble cytoplasmic inclusions (4,32,34). These aggregates sequester wild-type, nuclear TDP-43, thus depleting TDP-43 from the nucleus (4). Since a recent study has shown that the N-terminal domain of TDP-43 alone is capable of oligomer formation *in vitro* (35), we examined whether the extreme N-terminus of TDP-43 influences TDP-43 aggregation in cultured cells and primary neurons. Consistent with previous reports (4,32,34), TDP-43 cytoplasmic inclusions were formed in cells expressing the TDP-43_{NLSm}. However, TDP-43_{NLSm} lacking extreme N-terminal residues (TDP-$43_{10-414\text{-}NLSm}$) or bearing mutations to key N-terminal residues (TDP-$43_{R6GV7GT8GE9G}$) showed diffuse cytoplasmic distribution. Of note, inclusions formed by TDP-43_{NLSm} sequestered TDP-43_{WT}. In contrast, given the inability of TDP-$43_{10-414\text{-}NLSm}$ and TDP-$43_{R6GV7GT8GE9G}$ to aggregate, sequestration of TDP-43_{WT} was not possible. Moreover, expression of GFP-TDP-43_{NLSm}, but not of GFP-TDP-$43_{10-414\text{-}NLSm}$ or GFP-TDP-$43_{R6GV7GT8GE9G\text{-}NLSm}$, resulted in a reduction of neurite outgrowth. These results suggest that the extreme N-terminal region of TDP-43 is required for the aggregation of full-length TDP-43, a consequence of which is impaired neurite outgrowth.

Taken together, we shed new light on the functions of TDP-43's extreme N-terminus under physiological and pathological conditions. Our findings indicate that the extreme N-terminal region of TDP-43 is crucial for maintaining the normal conformation and biological activity of TDP-43 under physiological conditions. In disease, however, TDP-43 accumulates in the cytosol, perhaps in response to various stressors (36,37). Once in the cytosol, our data would suggest that the extreme N-terminal region of TDP-43 mediates full-length TDP-43 oligomerization and aggregate formation. This would result in a loss of functional TDP-43 due to sequestration of wild-type TDP-43 into insoluble inclusions, and perhaps a toxic gain of function resulting from the generation of TDP-43 oligomers and aggregates. In summary, we have uncovered an intriguing dichotomy: the extreme N-terminal region of TDP-43 regulates normal TDP-43 structure and function, but it may also participate in driving neurodegeneration in TDP-43 proteinopathies.

MATERIALS AND METHODS

Computer-assisted modeling of TDP-43 structures

The studies of computer-assisted modeling of TDP-43 structures are detailed in Supplementary Material.

Generation of TDP-43 plasmids

Full-length human TDP-43 complementary DNA (cDNA) from GFP-TDP-43 constructs (14) was used as the PCR template to generate N-terminal deleted TDP-43 constructs. The cDNA of fragments encoding TDP-43_{5-414}, TDP-43_{10-414}, TDP-43_{15-414}, TDP-43_{31-414}, TDP-43_{46-414} and TDP-43_{61-414} was generated by PCR. The upstream primers were: TDP-43_{5-414}: 5′-CGGGATCCATGATTCGGGTAACCGAAGA TGAG-3′; TDP-43_{10-414}: 5′-CGGGATCCATGGATGAGAA CGATGAGCCCATTG-3′; TDP-43_{15-414}: 5′-CGGGATCCA TGCCCATTGAAATACCATCGG-3′; TDP-43_{31-414}: 5′-CGGGATCCATGGTTACAGCCCAGTTTCCAGG-3′; TDP-43_{46-414}: 5′-CGGGATCCATGCCAGTGTCTCAGTGTA TGAG-3′; TDP-43_{61-414}: 5′-CGGGATCCATGCTGCATGCC CCAGATGCTGG-3′. The downstream primer was 5′-GCTCT AGACTACATTCCCCAGCCAGAAGAC-3′; The PCR product was sub-cloned into the pEGFP-C1 vector (N-terminally GFP-tagged, Clontech) or pcDNA5/TO (untagged, Invitrogen) using restriction sites BamHI and XbaI. The primers for PAG-3 plasmids encoding untagged TDP-43 were: wild-type TDP-43: 5′-AGTGAAGCTTGCCACCATGTCTGAATATATTCGG-3′ and 5′-TCATCTCGAGCTACATTCCCCAGCCAGAAG-3′; TDP-43_{1-273}: 5′-AGTGAAGCTTGCCACCATGTCTGAATA TATTCGG-3′ and 5′-TCATCTCGAGCTAACTTCTTTCTAA CTGTC-3′; TDP-43_{10-414}: 5′-AGTGAAGCTTGCCACCATGG ATGAGAACGATGAGCCC-3′ and 5′-TCATCTCGAGCTA CATTCCCCAGCCAGAAG-3′; TDP-43_{76-414}: 5′-AGTG AAGCTTGCCACCATGAACTATCCAAAAGATAAC-3′ and 5′-TCATCTCGAGCTACATTCCCCAGCCAGAAG-3′. The sequence of all plasmids was verified by sequence analysis.

Site-directed mutagenesis of TDP-43

Site-directed mutagenesis was performed using a Quikchange kit (Strategene). Wild-type TDP-43 in the pcDNA5/TO vector was used as a template to create the TDP-43 mutants. The primers used were: S2A: 5′- GAGCTCGGATCCATGGCTG AATATATTCGG-3′ and 5′-CCGAATATATTCAGCCATG GATCCGAGCTC-3′; S2D: 5′-CCGAGCTCGGATCCATGG ATGAATATATTCGGGTAAC-3′ and 5′-GTTACCCGAAT ATATTCATCCATGGATCCGAGCTCGG-3′; Y4F: 5′-GGA TCCATGTCTGAATTTATTCGGGTAACCGAAG-3′ and 5′-CTTCGGTTACCCGAATAAATTCAGACATGGATCC-3′; Y4D: 5′-GATCCATGTCTGAAGATATTCGGGTAACCG-3′ and 5′-CGGTTACCCGAATATCTTCAGACATGGATC-3′; Y4FT8A: 5′-CATGTCTGAATTTATTCGGGTAGCCGAAG

ATGAGAACGA-3′ and 5′-TCGTTCTCATCTTCGGCTACCC GAATAAATTCAGACATG-3′; Y4DT8E: 5′- ATGTCTGAA GATATTCGGGTAGAGGAAGATGAGAACGATGAGCCC-3′ and 5′-GGGCTCATCGTTCTCATCTTCCTCTACCCGAATA TCTTCAGACAT-3′; R6GV7G: 5′-CTCGGATCCATGTCTGA ATATATTGGGGGAACCGAAGATGAG-3′ and 5′-CTCATC TTCGGTTCCCCCAATATATTCAGACATGGATCCGAG-3′; R6GV7GT8GE9G: 5′-CATGTCTGAATATATTGGGGGAGG CGGAGATGAGAACGATGAGCC-3′ and 5′-GGCTCATCGT TCTCATCTCCGCCTCCCCCAATATATTCAGACATG-3′. The mutations were verified by sequence analysis.

In-cell cross-linking

In-cell cross-linking was performed by using DSG as previously described (38). DSG is a membrane-permeable small molecule widely used to stabilize the native structures of proteins (24–28) and protein–DNA complexes (39–42) in living cells, and can thus gain access to the nucleus by passive diffusion to stabilize TDP-43 homodimers. In brief, HEK293T, HeLa and M17 cells were harvested and washed twice with ice-cold phosphate-buffered saline (PBS, pH 7.4). Cells were re-suspended in 100 μl PBS. DSG (ProteoChem, Inc, c1104) stocks were prepared in dry DMSO. The reaction was initiated by adding 1 μl of a DSG stock to the 100 μl cell suspension at a final concentration of 12.5, 25, 50 or 100 μM. After 30 min of shacking at room temperature, the reaction was quenched by adding 2 μl of 1M Tris base solution at a final concentration of 20 mM for 15 min. Cells were then lysed in buffer (50 mM Tris–HCl, pH 7.4, 300 mM NaCl, 1% Triton-X-100, 5 mM EDTA, 1% SDS, plus phenylmethylsulfonyl fluoride (PMSF) and both a protease and phosphatase inhibitor mixture). After centrifugation at 16 000*g* for 20 min at 4°C, the supernatant was saved for western blot analysis. To map the critical protein sequence for TDP-43 homodimerization, HEK293T cells were transected with 1 μg wild-type TDP-43, TDP-43 fragments (TDP-43_{1-274}, TDP-43_{10-414} or TDP-43_{76-414}) or TDP-43 mutants (TDP-43_{Y4FT8A}, TDP-43_{Y4DT8E}, TDP-43_{R6GV7G} or TDP-$43_{R6GV7GT8GE9G}$) using Lipofectamine 2000 (Invitrogen) according to the manufacturer's instructions. Four hours after transfection, cells were treated with siTDP-43 targeting the 3′ UTR of endogenous TDP-43. Forty-eight hours post-treatment, cells were harvested for in-cell cross-linking, as described above.

Cell culture and Immunofluorescence

HEK293T cells grown on glass coverslips were transfected with 0.3 μg of an expression vector (GFP-TDP-43_{NLSm}, GFP-TDP-$43_{10-414NLSm}$) in the absence or presence of TDP-43-Myc (0.5 μg) using Lipofectamine 2000 (Invitrogen). Twenty-four hours post-transfection, cells were fixed with 4% paraformaldehyde in PBS (4°C, 15 min) and permeabilized with PBS-0.5% Triton X-100 for 10 min. After blocking with 5% non-fat milk for 1 h at 37°C, the cells were incubated overnight at 4°C with mouse monoclonal anti-Myc (1:500, Roche, 9E10). After washing, the cells were incubated with the Alexa 568-conjugated donkey anti-mouse secondary antibody (1:500, Molecular Probes) at 37°C for 2 h. To determine whether DSG treatment induces the mislocalization of TDP-43, HEK293T cells were treated with DSG (100 μM) for 30 min. The reaction was quenched by a Tris base, and the cells were subjected to immunofluorescence analysis using the rabbit polyclonal TDP-43 antibody (1:2000, Proteintech, 12892-1-AP) and the Alexa Fluor 488-conjugated donkey anti-rabbit secondary antibody (1:1000, Molecular Probes). Hoechst 33258 (1 μg/ml, Invitrogen) was used to stain cellular nuclei. Images were obtained on a Zeiss LSM 510 META confocal microscope.

Western blot analysis

Samples were prepared in Laemmli's buffer, heated for 5 min at 95°C, and equal amounts of protein were loaded into 3–8% Tris–acetate gels for TDP-43 analysis, 4–20% Tris–glycine gels for DJ-1 analysis or 10% Tris–glycine gels for other proteins of interest. After transfer, blots were blocked with 5% nonfat dry milk in Tris-buffered saline - 0.1% Triton X-100 (TBST) for 1 h, then incubated with a rabbit polyclonal GFP antibody (1:2000, Invitrogen), rabbit polyclonal TDP-43 (Proteintech, 10728-2-AP), rabbit polyclonal TDP-43 antibody (Proteintech, 12892-1-AP), rabbit DJ-1antibody (Cell Signaling, #5933), mouse monoclonal hnRNP-A2 antibody (Sigma, R4653) or mouse monoclonal GAPDH antibody (1:10000, Biodesign) overnight at 4°C. Membranes were washed in TBST, then incubated with donkey anti-rabbit, anti-mouse or anti-goat IgG conjugated to horseradish peroxidase (1:5000; Jackson ImmunoResearch) for 1 h. Protein expression was visualized by enhanced chemiluminescence treatment and exposure to a film.

RNA extraction and semi-quantitative RT–PCR

The *CFTR* mini-gene splicing assay was conducted as previously described (14,43). In brief, HeLa cells were co-transfected with 1 μg of a mini-gene construct and 1 or 2 μg of GFP-TDP-43 constructs or untagged TDP-43 constructs. After 48 h, the cells were harvested and total RNA was extracted using the RNeasy Plus Mini kit (Qiagen). Then, 2 μg of total RNA was used to synthesize cDNA with the High Capacity cDNA Reverse Transcription kit (Applied Biosystems). For the PCR, 2 μl of cDNA was used in a 20 μl of reaction according to the manufacturer's protocol for a Taq PCR Core kit (Qiagen). The amplification conditions consisted of an initial denaturation step at 94°C for 3 min, followed by 30 cycles of 94°C for 30 s, 62°C for 60 s, and 72°C for 90 s. The PCR products were run on 1% agarose gels for 30 min at 135 volts.

Immunoprecipitation

For immunoprecipitation studies, HEK293T cells were treated with 100 μM DSG and cells were lysed using Co-IP buffer (50 mM Tris–HCl, pH 7.4, 300 mM NaCl, 1% Triton X-100, 5 mM EDTA) containing PMSF as well as protease and phosphatase inhibitors. Lysates were sonicated and centrifuged at 16 000*g* for 20 min. The protein concentration of supernatants was determined by BCA assay (Thermo Scientific). The supernatant containing 300 μg of total protein was pre-cleaned with Dynabeads® Protein G (Invitrogen), and

then combined with 1.5 μl of anti-TDP-43 antibody (Proteintech, 12892-1-AP) and incubated overnight at 4°C with gentle shaking. The antigen–antibody immunocomplex was captured by Dynabeads® Protein G (Invitrogen) for 4 h, and then the beads were pulled-down using a Tube Magnetic Stand (Invitrogen). The beads were washed with Co-IP buffer, and captured proteins eluted from the beads using loading buffer was resolved by SDS–PAGE for western blot analysis using a monoclonal TDP-43 antibody (Proteintech, 60019-2-Ig). Co-immunoprecipitation experiments were performed as previously described (14). In brief, HEK293T cells were cotransfected with 2 μg Flag-TDP-43 and 1 μg of vector for GFP-TDP-43, GFP-TDP-43_{1-273}, GFP-TDP-43_{10-414}, or GFP-TDP-43_{76-414} expression. The supernatant containing 300 μg of total protein was incubated with Anti-Flag M2 agarose (Sigma) overnight at 4°C with gentle shaking. Captured proteins eluted from the beads using loading buffer were subjected to western blot analysis.

Primary neuronal culture

The cortex from embryonic day 18 (E18) mouse pups were dissected in HIBERNATE™ A media without calcium (BrainBits), and then incubated in 1 mg/ml papain (Fisher Scientific) at 30°C for 30 min. Tissue was dissociated by triturating with a series of Pasteur pipettes of decreasing diameter. Following centrifugation to collect the cell pellet, the cells were resuspended in Neurobasal A (Invitrogen) supplemented with B27, GMAX, gentamicin and bFGF (Invitrogen). Neurons were seeded at a density of 2×10^4 cells/coverslip in 24-well plates for immunofluorescence studies. At day *in vitro* 4, 1×10^9 genome rAAV1 virus of GFP, GFP-TDP-43_{NLSm}, GFP-TDP-$43_{10-414\text{-}NLSm}$ or GFP-TDP-$43_{R6GV7GT8GE9G\text{-}NLSm}$ was added to the cell medium. Five days later, neurons were fixed and immunostained using a mouse monoclonal MAP2 antibody (1:1000, Sigma). All rAAV1 vectors were prepared by standard methods, as previously described (44).

Quantification of neurite outgrowth

Quantification of neurite outgrowth was performed as previously described (44). In brief, images of neurons were captured using a Zeiss LSM 510 META confocal microscope and neurite outgrowth (50 neurons for each treatment) was measured using MetaMorph version 7.1 (Molecular Devices, Downingtown, PA, USA). Data from three separate experiments were analyzed by one-way analysis of variance followed by Tukey's *post-hoc* analysis ($^{***}P < 0.001$).

AUTHORS' CONTRIBUTION

Y.Z., Y.X., J.H., H.S., E.C.W., S.H. and W.C.L. performed experiments. TC performed computer-assisted modeling of TDP-43 monomeric and dimeric structures. Y.Z., T.G., and L.P. performed data analysis. Y.Z., T.G., C.S. and L.P. wrote the manuscript. Y.Z. and L.P. conceived of the study, participated in its design and coordination and edited the manuscript. All authors read and approved the final manuscript.

SUPPLEMENTARY MATERIAL

Supplementary Material is available at *HMG* online.

ACKNOWLEDGEMENTS

Dr Francisco Baralle and Dr Emanuele Buratti kindly provided the *CFTR* mini-gene which was used in our previous studies (14).

Conflict of Interest statement. None declared.

FUNDING

This work was supported by Mayo Clinic Foundation to L.P., National Institutes of Health/National Institute on Aging (R01AG026251 to L.P.), National Institutes of Health/National Institute of Neurological Disorders and Stroke (R01 NS 063964-01 to L.P., R01 NS077402 to L.P., ES20395-01 to L.P., R21 NS074121-01 to T.F.G., 1R21NS079807-01A1 to Y.Z.), Amyotrophic Lateral Sclerosis Association to L.P., GHR Foundation to Y.Z, and the Department of Defense (W81XWH-10-1-0512-1 to L.P. and W81XWH-09-1-0315AL093108 to L.P.). Funding to pay the Open Access publication charges for this article was provided by Mayo Clinic (Department of Neuroscience).

REFERENCES

1. Arai, T., Hasegawa, M., Akiyama, H., Ikeda, K., Nonaka, T., Mori, H., Mann, D., Tsuchiya, K., Yoshida, M., Hashizume, Y. *et al.* (2006) TDP-43 is a component of ubiquitin-positive tau-negative inclusions in frontotemporal lobar degeneration and amyotrophic lateral sclerosis. *Biochem. Biophys. Res. Commun.*, **351**, 602–611.
2. Neumann, M., Sampathu, D.M., Kwong, L.K., Truax, A.C., Micsenyi, M.C., Chou, T.T., Bruce, J., Schuck, T., Grossman, M., Clark, C.M. *et al.* (2006) Ubiquitinated TDP-43 in frontotemporal lobar degeneration and amyotrophic lateral sclerosis. *Science*, **314**, 130–133.
3. Buratti, E. and Baralle, F.E. (2008) Multiple roles of TDP-43 in gene expression, splicing regulation, and human disease. *Front Biosci.*, **13**, 867–878.
4. Winton, M.J., Igaz, L.M., Wong, M.M., Kwong, L.K., Trojanowski, J.Q. and Lee, V.M. (2008) Disturbance of nuclear and cytoplasmic TAR DNA-binding protein (TDP-43) induces disease-like redistribution, sequestration, and aggregate formation. *J. Biol. Chem.*, **283**, 13302–13309.
5. Ayala, Y.M., Pantano, S., D'Ambrogio, A., Buratti, E., Brindisi, A., Marchetti, C., Romano, M. and Baralle, F.E. (2005) Human, Drosophila, and C. elegans TDP43: nucleic acid binding properties and splicing regulatory function. *J. Mol. Biol.*, **348**, 575–588.
6. Buratti, E. and Baralle, F.E. (2001) Characterization and functional implications of the RNA binding properties of nuclear factor TDP-43, a novel splicing regulator of CFTR exon 9. *J. Biol. Chem.*, **276**, 36337–36343.
7. Buratti, E., Brindisi, A., Giombi, M., Tisminetzky, S., Ayala, Y.M. and Baralle, F.E. (2005) TDP-43 binds heterogeneous nuclear ribonucleoprotein A/B through its C-terminal tail: an important region for the inhibition of cystic fibrosis transmembrane conductance regulator exon 9 splicing. *J. Biol. Chem.*, **280**, 37572–37584.
8. Gitcho, M.A., Baloh, R.H., Chakraverty, S., Mayo, K., Norton, J.B., Levitch, D., Hatanpaa, K.J., White, C.L. 3rd, Bigio, E.H., Caselli, R. *et al.* (2008) TDP-43 A315T mutation in familial motor neuron disease. *Ann. Neurol.*, **63**, 535–538.
9. Kabashi, E., Valdmanis, P.N., Dion, P., Spiegelman, D., McConkey, B.J., Vande Velde, C., Bouchard, J.P., Lacomblez, L., Pochigaeva, K., Salachas, F. *et al.* (2008) TARDBP mutations in individuals with sporadic and familial amyotrophic lateral sclerosis. *Nat. Genet.*, **40**, 572–574.

10. Rutherford, N.J., Zhang, Y.J., Baker, M., Gass, J.M., Finch, N.A., Xu, Y.F., Stewart, H., Kelley, B.J., Kuntz, K., Crook, R.J. *et al.* (2008) Novel mutations in TARDBP (TDP-43) in patients with familial amyotrophic lateral sclerosis. *PLoS Genet.*, **4**, e1000193.
11. Sreedharan, J., Blair, I.P., Tripathi, V.B., Hu, X., Vance, C., Rogelj, B., Ackerley, S., Durnall, J.C., Williams, K.L., Buratti, E. *et al.* (2008) TDP-43 mutations in familial and sporadic amyotrophic lateral sclerosis. *Science*, **319**, 1668–1672.
12. Yokoseki, A., Shiga, A., Tan, C.F., Tagawa, A., Kaneko, H., Koyama, A., Eguchi, H., Tsujino, A., Ikeuchi, T., Kakita, A. *et al.* (2008) TDP-43 mutation in familial amyotrophic lateral sclerosis. *Ann. Neurol.*, **63**, 538–542.
13. Igaz, L.M., Kwong, L.K., Chen-Plotkin, A., Winton, M.J., Unger, T.L., Xu, Y., Neumann, M., Trojanowski, J.Q. and Lee, V.M. (2009) Expression Of TDP-43 C-terminal fragments in vitro recapitulates pathological features of TDP-43 proteinopathies. *J. Biol. Chem.*, **284**, 8516–8524.
14. Zhang, Y.J., Xu, Y.F., Cook, C., Gendron, T.F., Roettges, P., Link, C.D., Lin, W.L., Tong, J., Castanedes-Casey, M., Ash, P. *et al.* (2009) Aberrant cleavage of TDP-43 enhances aggregation and cellular toxicity. *Proc. Natl. Acad. Sci. U S A.*, **106**, 7607–7612.
15. Nonaka, T., Kametani, F., Arai, T., Akiyama, H. and Hasegawa, M. (2009) Truncation and pathogenic mutations facilitate the formation of intracellular aggregates of TDP-43. *Hum. Mol. Genet.*, **18**, 3353–3364.
16. Fuentealba, R.A., Udan, M., Bell, S., Wegorzewska, I., Shao, J., Diamond, M.I., Weihl, C.C. and Baloh, R.H. (2010) Interaction with polyglutamine aggregates reveals a Q/N-rich domain in TDP-43. *J. Biol. Chem.*, **285**, 26304–26314.
17. Budini, M., Buratti, E., Stuani, C., Guarnaccia, C., Romano, V., De Conti, L. and Baralle, F.E. (2012) Cellular model of TAR DNA-binding protein 43 (TDP-43) aggregation based on its C-terminal Gln/Asn-rich region. *J. Biol. Chem.*, **287**, 7512–7525.
18. Ling, S.C., Albuquerque, C.P., Han, J.S., Lagier-Tourenne, C., Tokunaga, S., Zhou, H. and Cleveland, D.W. (2010) ALS-associated mutations in TDP-43 increase its stability and promote TDP-43 complexes with FUS/TLS. *Proc. Natl Acad. Sci. USA*, **107**, 13318–13323.
19. Johnson, B.S., Snead, D., Lee, J.J., McCaffery, J.M., Shorter, J. and Gitler, A.D. (2009) TDP-43 is intrinsically aggregation-prone, and amyotrophic lateral sclerosis-linked mutations accelerate aggregation and increase toxicity. *J. Biol. Chem.*, **284**, 20329–20339.
20. Kuo, P.H., Doudeva, L.G., Wang, Y.T., Shen, C.K. and Yuan, H.S. (2009) Structural insights into TDP-43 in nucleic-acid binding and domain interactions. *Nucleic Acids Res.*, **37**, 1799–1808.
21. Buratti, E., Dork, T., Zuccato, E., Pagani, F., Romano, M. and Baralle, F.E. (2001) Nuclear factor TDP-43 and SR proteins promote in vitro and in vivo CFTR exon 9 skipping. *EMBO J.*, **20**, 1774–1784.
22. Polymenidou, M., Lagier-Tourenne, C., Hutt, K.R., Huelga, S.C., Moran, J., Liang, T.Y., Ling, S.C., Sun, E., Wancewicz, E., Mazur, C. *et al.* (2011) Long pre-mRNA depletion and RNA missplicing contribute to neuronal vulnerability from loss of TDP-43. *Nat. Neurosci.*, **14**, 459–468.
23. Tollervey, J.R., Curk, T., Rogelj, B., Briese, M., Cereda, M., Kayikci, M., Konig, J., Hortobagyi, T., Nishimura, A.L., Zupunski, V. *et al.* (2011) Characterizing the RNA targets and position-dependent splicing regulation by TDP-43. *Nat. Neurosci.*, **14**, 452–458.
24. Bartels, T., Choi, J.G. and Selkoe, D.J. (2011) alpha-Synuclein occurs physiologically as a helically folded tetramer that resists aggregation. *Nature*, **477**, 107–110.
25. Leitner, A., Walzthoeni, T., Kahraman, A., Herzog, F., Rinner, O., Beck, M. and Aebersold, R. (2010) Probing native protein structures by chemical cross-linking, mass spectrometry, and bioinformatics. *Mol. Cell Proteomics*, **9**, 1634–1649.
26. Canet-Aviles, R.M., Wilson, M.A., Miller, D.W., Ahmad, R., McLendon, C., Bandyopadhyay, S., Baptista, M.J., Ringe, D., Petsko, G.A. and Cookson, M.R. (2004) The Parkinson's disease protein DJ-1 is neuroprotective due to cysteine-sulfinic acid-driven mitochondrial localization. *Proc. Natl Acad. Sci. USA*, **101**, 9103–9108.
27. Rapaport, D. and Neupert, W. (1999) Biogenesis of Tom40, core component of the TOM complex of mitochondria. *J. Cell Biol.*, **146**, 321–331.
28. Lo, K.W., Kan, H.M. and Pfister, K.K. (2006) Identification of a novel region of the cytoplasmic Dynein intermediate chain important for dimerization in the absence of the light chains. *J. Biol. Chem.*, **281**, 9552–9559.
29. Dettmer, U., Newman, A.J., Luth, E.S., Bartels, T. and Selkoe, D. (2013) In vivo cross-linking reveals principally oligomeric forms of alpha-synuclein and beta-synuclein in neurons and non-neural Cells. *J. Biol. Chem.*, **288**, 6371–6385.
30. Repici, M., Straatman, K.R., Balduccio, N., Enguita, F.J., Outeiro, T.F. and Giorgini, F. (2012) Parkinson's disease-associated mutations in DJ-1 modulate its dimerization in living cells. *J. Mol. Med. (Berl)*. [Epub ahead of print].
31. Deeg, S., Gralle, M., Sroka, K., Bahr, M., Wouters, F.S. and Kermer, P. (2010) BAG1 restores formation of functional DJ-1 L166P dimers and DJ-1 chaperone activity. *J. Cell Biol.*, **188**, 505–513.
32. Elden, A.C., Kim, H.J., Hart, M.P., Chen-Plotkin, A.S., Johnson, B.S., Fang, X., Armakola, M., Geser, F., Greene, R., Lu, M.M. *et al.* (2010) Ataxin-2 intermediate-length polyglutamine expansions are associated with increased risk for ALS. *Nature*, **466**, 1069–1075.
33. Fiesel, F.C., Voigt, A., Weber, S.S., Van den Haute, C., Waldenmaier, A., Gorner, K., Walter, M., Anderson, M.L., Kern, J.V., Rasse, T.M. *et al.* (2010) Knockdown of transactive response DNA-binding protein (TDP-43) downregulates histone deacetylase 6. *EMBO J.*, **29**, 209–221.
34. Barmada, S.J., Skibinski, G., Korb, E., Rao, E.J., Wu, J.Y. and Finkbeiner, S. (2010) Cytoplasmic mislocalization of TDP-43 is toxic to neurons and enhanced by a mutation associated with familial amyotrophic lateral sclerosis. *J. Neurosci.*, **30**, 639–649.
35. Chang, C.K., Wu, T.H., Wu, C.Y., Chiang, M.H., Toh, E.K., Hsu, Y.C., Lin, K.F., Liao, Y.H., Huang, T.H. and Huang, J.J. (2012) The N-terminus of TDP-43 promotes its oligomerization and enhances DNA binding affinity. *Biochem. Biophys. Res. Commun.*, **425**, 219–224.
36. Cohen, T.J., Lee, V.M. and Trojanowski, J.Q. (2011) TDP-43 functions and pathogenic mechanisms implicated in TDP-43 proteinopathies. *Trends Mol. Med.*, **17**, 659–667.
37. Polymenidou, M. and Cleveland, D.W. (2011) The seeds of neurodegeneration: prion-like spreading in ALS. *Cell*, **147**, 498–508.
38. Fauvet, B., Mbefo, M.K., Fares, M.B., Desobry, C., Michael, S., Ardah, M.T., Tsika, E., Coune, P., Prudent, M., Lion, N. *et al.* (2012) alpha-synuclein in central nervous system and from erythrocytes, mammalian cells, and Escherichia coli exists predominantly as disordered monomer. *J. Biol. Chem.*, **287**, 15345–15364.
39. Nowak, D.E., Tian, B. and Brasier, A.R. (2005) Two-step cross-linking method for identification of NF-kappaB gene network by chromatin immunoprecipitation. *Biotechniques*, **39**, 715–725.
40. Ramadoss, P., Unger-Smith, N.E., Lam, F.S. and Hollenberg, A.N. (2009) STAT3 targets the regulatory regions of gluconeogenic genes in vivo. *Mol. Endocrinol.*, **23**, 827–837.
41. Chen, H., Kluz, T., Zhang, R. and Costa, M. (2010) Hypoxia and nickel inhibit histone demethylase JMJD1A and repress Spry2 expression in human bronchial epithelial BEAS-2B cells. *Carcinogenesis*, **31**, 2136–2144.
42. Gillespie, R.F. and Gudas, L.J. (2007) Retinoid regulated association of transcriptional co-regulators and the polycomb group protein SUZ12 with the retinoic acid response elements of Hoxa1, RARbeta(2), and Cyp26A1 in F9 embryonal carcinoma cells. *J. Mol. Biol.*, **372**, 298–316.
43. Pagani, F., Buratti, E., Stuani, C., Romano, M., Zuccato, E., Niksic, M., Giglio, L., Faraguna, D. and Baralle, F.E. (2000) Splicing factors induce cystic fibrosis transmembrane regulator exon 9 skipping through a nonevolutionary conserved intronic element. *J. Biol. Chem.*, **275**, 21041–21047.
44. Gass, J., Lee, W.C., Cook, C., Finch, N., Stetler, C., Jansen-West, K., Lewis, J., Link, C.D., Rademakers, R., Nykjaer, A. *et al.* (2012) Progranulin regulates neuronal outgrowth independent of Sortilin. *Mol. Neurodegener.*, **7**, 33.